The Journal of Immunology

Y-Box Binding Protein-1 Mediates Profibrotic Effects of Calcineurin Inhibitors in the Kidney

Lydia Hanssen, Björn C. Frye, Tammo Ostendorf, Christina Alidousty, Sonja Djudjaj, Peter Boor, Thomas Rauen, Jürgen Floege, Peter R. Mertens and Ute Raffetseder

J Immunol 2011; 187:298-308; Prepublished online 23 May 2011;
doi: 10.4049/jimmunol.1100382
http://www.jimmunol.org/content/187/1/298

The Journal of Immunology is published twice each month by
The American Association of Immunologists, Inc.,
1451 Rockville Pike, Suite 650, Rockville, MD 20852

Print ISSN: 0022-1767 Online ISSN: 1550-6606.

Y-Box Binding Protein-1 Mediates Profibrotic Effects of Calcineurin Inhibitors in the Kidney

Lydia Hanssen,* Björn C. Frye,* Tammo Ostendorf,* Christina Alidousty,* Sonja Djudjaj,* Peter Boor,*,†,‡ Thomas Rauen,* Jürgen Floege,* Peter R. Mertens,§ and Ute Raffetseder*

The immunosuppressive calcineurin inhibitors (CNIs) cyclosporine A (CsA) and tacrolimus are widely used in transplant organ recipients, but in the kidney allograft, they may cause tubulointerstitial as well as mesangial fibrosis, with TGF-β believed to be a central inductor. In this study, we report that the cold-shock protein Y-box binding protein-1 (YB-1) is a TGF-β independent downstream effector in CsA- as well as in tacrolimus- but not in rapamycin-mediated activation of rat mesangial cells (rMCs). Intracellular content of YB-1 is several-fold increased in MCs following CNI treatment in vitro and in vivo in mice. This effect ensues in a time-dependent manner, and the operative concentration range encompasses therapeutically relevant doses for CNIs. The effect of CNI on cellular YB-1 content is abrogated by specific blockade of translation, whereas retarding the transcription remains ineffective. The activation of rMCs by CNIs is accomplished by generation of reactive oxygen species. In contrast to TGF-β–triggered reactive oxygen species generation, hydrogen peroxide especially could be identified as a potent inductor of YB-1 accumulation. In line with this, hindering TGF-β did not influence CNI-induced YB-1 upregulation, whereas ERK/Akt pathways are involved in CNI-mediated YB-1 expression. CsA-induced YB-1 accumulation results in mRNA stabilization and subsequent generation of collagen. Our results provide strong evidence for a CNI-dependent induction of YB-1 in MCs that contributes to renal fibrosis via regulation of its own and collagen translation. ***The Journal of Immunology*****, 2011, 187: 298–308.**

Immunosuppressive agents such as calcineurin inhibitors (CNIs) cyclosporine A (CsA) and tacrolimus (Tac) have contributed to a substantial improvement of allograft survival. These pharmaceuticals are integral parts of standard therapy regimens to prevent allograft rejection (1, 2), thereby increasing 2-y graft survival rates from 48 to 76% after cadaveric renal transplantation (3). Despite their beneficial effects on allograft survival, CNIs also exert nephrotoxic side effects contributing to acute or chronic allograft nephropathy. Acute CNI nephrotoxicity is due to hemodynamic alterations caused by vasoconstriction of the afferent arterioles that eventually leads to a decreased glomerular filtration rate. Chronic nephrotoxicity is characterized by arteriolar hyalinosis, increased glomerulosclerosis, and tubulointerstitial damage (4). These observations account for the large clinical interest in the development of CNI-sparing regimens (5).

The fibrogenic effect of CNIs in the renal allograft is predominantly mediated by elevated intrarenal expression of TGF-β (6, 7) and subsequent excessive extracellular matrix (ECM) generation (8, 9). In mesangial cells (MCs), TGF-β stimulates the synthesis of collagen type 1 (Col1A) (10), and application of anti–TGF-β Abs in CsA-treated rats reversed the majority, albeit not all, of CNI-associated renal lesions (11). Besides TGF-β, a variety of other mediators have been identified to initiate or modify intracellular signaling pathways that lead to ECM accumulation, such as platelet-derived growth factor (12) and connective tissue growth factor (13). Recently, reactive oxygen species (ROS) has been shown to activate latent TGF-β in rat MCs (rMCs), important producers of extracellular Col1A in glomeruli (14). However, despite some knowledge on mediators of CNI nephrotoxicity, the sequences of pathophysiological events need to be defined more precisely.

The highly conserved Y-box binding protein-1 (YB-1) belongs to the family of cold-shock proteins that is of particular relevance in situations of cellular stress responses. Various studies point to the mitogenic propensities of YB-1, either beneficial to health and development (15) or with pathological potential during tumorigenesis (16). With its capacity to exhibit RNA- as well as DNA-binding properties, YB-1 controls the cellular content of multiple proteins. By means of RNA binding, YB-1 protects IL-2 and GM-CSF mRNA from degradation and controls TGF-β1 translation in proximal tubular cells (17). Furthermore, YB-1 is involved in mRNA processing (18).

As a key regulator of gene transcription, YB-1 mediates expression of genes that are involved in ECM turnover such as Col1A (19) and matrix metalloproteinase-2 (MMP-2) (20). Recent findings from our group indicate that YB-1 plays a significant role in coordinating immune cell chemotaxis, as it serves as a potent

*Department of Nephrology and Clinical Immunology, University Hospital Rheinisch-Westfälische Technische Hochschule-Aachen, Aachen 52057, Germany; †Institute of Pathology, University Hospital Rheinisch-Westfälische Technische Hochschule-Aachen, Aachen 52057, Germany; ‡Institute of Molecular Biomedicine, Comenius University, Bratislava 81806, Slovakia; and §Department of Nephrology and Hypertension, Otto-von-Guericke University Magdeburg, Magdeburg 39106, Germany

Received for publication February 4, 2011. Accepted for publication April 20, 2011.

This work was supported by the Else-Kröner-Fresenius-Stiftung (to U.R.) and Sonderforschungsbereich 542 Projects C4 (to P.R.M.) and C12 (to U.R. and P.R.M.).

Address correspondence and reprint requests to Dr. Ute Raffetseder, Department of Nephrology and Clinical Immunology, University Hospital Rheinisch-Westfälische Technische Hochschule-Aachen, Pauwelsstrasse 30, Aachen 52057, Germany. E-mail address: uraffetseder@ukaachen.de

Abbreviations used in this article: Act.D, actinomycin D; Cat, catalase; CHX, cycloheximide; CNI, calcineurin inhibitor; Col1A, collagen type 1; CsA, cyclosporine A; DPI, diphenylene iodonium; Ebs, ebselen; ECM, extracellular matrix; HEK, human embryonic kidney; HK-2, human tubular kidney; hMC, human mesangial cell; HXXO, hypoxanthine/xanthine oxidase system; MC, mesangial cell; MMP-2, matrix metalloproteinase-2; mRNP, mRNA particle; Nac, *N*-acetylcysteine; PEG-SOD, polyethylene glycol-superoxide dismutase; qRT-PCR, quantitative real-time PCR; rMC, rat mesangial cell; ROS, reactive oxygen species; RT, room temperature; Tac, tacrolimus; YB-1, Y-box binding protein-1.

www.jimmunol.org/cgi/doi/10.4049/jimmunol.1100382

transcriptional *trans*-regulator of β-chemokine RANTES/CCL5 expression in monocytes/macrophages (21) as well as in human arterial smooth muscle cells (22). Thereby, YB-1 contributes to allotransplant rejection and is involved in accelerated atherosclerosis, as demonstrated in experimental animal models (21, 22).

In a model of acute mesangioproliferative glomerulonephritis (anti-Thy1.1 nephritis), YB-1 expression is upregulated in MCs in a time-dependent manner and mediates platelet-derived growth factor-B effects in renal cells (23, 24). Furthermore, YB-1 induces MC proliferation via activation of the ERK1/2 pathway (25) and acts as cell type-specific activator of MMP-2 gene expression in MCs (20). MMP-2 belongs to the family of zinc-dependent endopeptidases that controls collagen degradation in the kidney, and by this, MMP-2 possesses high relevance in fibrotic processes. Another active role of YB-1 in fibrosis is accomplished by transcriptional control of the cellular content of α-smooth muscle actin (26) and Col1A (19, 27–29). Furthermore, in proximal tubular cells, YB-1 controls TGF-β1 translation (17), the most potent and ubiquitous profibrotic cytokine.

Given the participation of YB-1 in fibrosis and immunological processes, we set out to investigate the role of YB-1 in calcineurin inhibitor-induced nephrotoxicity in MCs.

Materials and Methods

Cell culture

All cell lines were cultured in humidified air with 5% CO_2 content at 37°C except for WT5 cells, which were grown at 33°C. rMCs (20) and primary human MCs (hMCs) were cultured in RPMI 1640 supplemented with 10% FCS, 2 mM glutamine, 5 ng/ml insulin, 100 U/ml penicillin, and 100 U/ml streptomycin. Human embryonic kidney (HEK) 293T cells were incubated in high-glucose DMEM with 10% FBS, 1 mM sodium pyruvate, 10 mM MEM nonessential amino acids, 100 U/ml penicillin, and 100 U/ml streptomycin. Immortalized human tubular kidney (HK)-2 cells (18) were grown in high-glucose DMEM supplemented with 20% FCS, 2 mM glutamine, 10 μg/ml insulin, 1 mM sodium pyruvate, 10 mM MEM nonessential amino acids, 100 U/ml penicillin, and 100 U/ml streptomycin. The immortalized podocytic mouse cell line, WT5, has been described previously (30). Undifferentiated WT5 cells were maintained in RPMI 1640 supplemented with 10% FCS, 1% L-glutamine, 1% sodium bicarbonate, 10,000 U/ml IFN-γ, 100 U/ml penicillin, and 100 U/ml streptomycin. All cell-culture media and supplements were purchased from Life Technologies unless otherwise stated.

Cell challenge

For stimulation, 1×10^6 cells were seeded in 75 cm^2 cell-culture flasks and always grown in serum-reduced media with only 1% FCS for 24 h prior to challenge. Unless indicated otherwise, cells were stimulated for the indicated periods with 1 μM CsA (Axxora) or 0.01 μM Tac (Axxora), 0.05 μM rapamycin, or DMSO (both from AppliChem). To specify transcriptional and translational effects, rMCs were preincubated either with 10 μM cycloheximide (CHX) or 10 μM actinomycin D (Act.D) for 15 min prior to CsA stimulation.

To investigate mRNA stability, cells were preincubated with CsA for 30 min, and Act.D was applied for 0.5, 1, and 24 h. To investigate YB-1 protein stability under CsA treatment, cells were treated with CsA for 8 h and subsequently incubated with CHX for the indicated times. CHX and Act.D were purchased both from AppliChem. To determine the degradation rate of YB-1 protein upon CsA incubation, rMCs were treated either with 10 or 50 μM proteasomal inhibitor MG132 (Sigma-Aldrich) for the indicated periods. For costimulation, rMCs were preincubated with MG132 for 30 min prior to CsA incubation. To investigate the role of ROS during CsA stimulation, rMCs were treated for 4 h with 1 μM CsA together with one of the following ROS inhibitors: 5 mM *N*-acetylcysteine (Nac), 10 μM diphenylene iodonium (DPI), 10 μM ebselen (Ebs; Calbiochem), 100 U/ml polyethylene glycol-superoxide dismutase (PEG-SOD), or 500 U/ml catalase (Cat). The hypoxanthine (50 μM)/xanthine oxidase (8 U/ml) system (HXXO) served as positive control because it produces endogenous ROS. Nac, Cat, DPI, PEG-SOD, and HXXO were obtained from Sigma-Aldrich. H_2O_2 (Merck) application was performed for the stated times and indicated concentrations. To specify involved signaling pathways, rMCs were prestimulated either with 10 μM LY294006 (Calbiochem) or 10 μM UO126 (Cell Signaling Technology) for 1 h prior to CsA challenge. To define the impact of Akt phosphorylation, cells were pretreated for 15 min with LY294006 and then stimulated with CsA for 5 min, 4 h, and 8 h. TGF-β inhibition was ascertained by 60-min preincubation with 20 μg neutralizing monoclonal TGF-β Ab (R&D Systems).

Knockdown of endogenous YB-1 by small interfering RNA

rMCs were transfected with the empty vector pSuper or the pSuper vector harboring the sequence 5′-GGTCATCGCAACGAAGGTTTT-3′ (Oligo-Engine) as a tail-to-tail tandem repeat of bp 285–305 of the human YB-1 coding sequence in conjunction with G418 resistance plasmid pUHD15–1neo (BD Clontech) using FuGene6 (Roche), as described before (24). Two of these clones were used for further experiments (YB-1-K0/1 and YB-1-K0/2).

Nuclear and cytoplasmic cell extracts and Western blot analyses

Nuclear and cytoplasmic cell extracts were prepared as described previously (21). Extracts were stored at −80°C. Protein concentrations were determined by the Bio-Rad protein assay (Bio-Rad) using BSA as standard. Unless otherwise stated, 10 μg protein of cytoplasmic, nuclear, or whole-cell extracts were subjected to SDS-PAGE, and Western blotting was performed as described before (18). The following Abs were used: YB-1 (polyclonal Ab against protein C terminus; from http://www.antibodies-online.com), phospho–YB-1 (polyclonal peptide-derived Ab specific against protein-phosphorylated AKT site; from http://www.antibodies-online.com), phospho-SMAD2, ERK, or phospho-ERK (from Cell Signaling Technology). Blots of whole-cell lysates or cytoplasmatic extracts were reprobed with a monoclonal anti-GAPDH–specific Ab (Novus Biologicals), whereas blots of nuclear extracts were incubated with a polyclonal anti-CREB–specific Ab (Cell Signaling Technology) to ensure equal protein loading. Band intensities were quantified by Scion Image software, and after normalization against values determined for GAPDH/CREB, the YB-1 content in untreated cells was set as 1, and relative band intensities were calculated.

Quantitative real-time PCR and PCR

For quantitative real-time PCR (qRT-PCR), rMCs and YB-1 knockdown rMCs (YB-1-K0/1 and rMCs YB-1-K0/2) were seeded at 2×10^5 cells/well in six-well plates and cultured in serum-reduced medium for 24 h before CsA treatment. Total RNA was purified using the RNeasy Mini Kit (Qiagen) according to the manufacturer's protocol. First-strand cDNA was synthesized with Moloney-monkey leukemia virus reverse transcriptase (Invitrogen). qRT-PCR was carried out on the 7300 real-time PCR system (Applied Biosystems). TaqMan master mix and TaqMan primer sets were obtained for rat collagen type I (Rn01463848_m1), human YB-1 (Hs02742754_g1), and eukaryotic 18S rRNA (Hs99999901_s1) as an internal control from Applied Biosystems.

RT-PCR was performed with primer pairs for rat Col1A (5′-CCAATCTGGTTCCCTCCCACC-3′ and 5′-GTAAGGTTGAATGCACTTTTG-3′) YB-1 (5′-CAGCGCCGCCGACA-3′ and 5′-ATATCCGTTCCTTACATTGAACCATT-3′), and GAPDH (5′-ACCACAGTCCATGCCATCAC-3′ and 5′-TCCACCACCCTGTTGCTGTA-3′) at the following conditions: 30 cycles at 94°C for 30 s, 55°C for 60 s, and 72°C for 30 s. Products were separated on 1% agarose gel stained with ethidium bromide. Band intensities were quantified by Scion Image software.

Coimmunoprecipitation of mRNA associated with YB-1

Prior to immunoprecipitation, polyclonal anti–YB-1 Ab and irrelevant anti-rabbit IgG (Cell Signaling Technology) as negative control were covalently linked to protein A-Sepharose beads (50% suspension; Invitrogen). For this, 20 μg Ab was incubated with 300 μl protein A-Sepharose for 1 h at room temperature (RT). Pelleted beads (3000 × *g*, 5 min) were washed twice with sodium borate (0.1 M [pH 9]), and dimethylpimelidate (Sigma-Aldrich) was added at a final concentration of 20 mM. After 30 min incubation at RT, beads were spun down, washed once in ethanolamine (0.2 M, pH 8), and subsequently incubated for 2 h in ethanolamine at RT. Beads were separated from unbound Abs and resuspended in 120 μl PBS containing 0.03% sodium azide. Then, 20 μl protein A-Sepharose coupled either with polyclonal anti–YB-1 Ab or unspecific IgG was incubated with 150 μg cytoplasmic cell extract from CsA-stimulated or untreated rMCs for 1.5 h at 4°C in IPP buffer (20 mM HEPES [pH 7.4], 100 mM potassium chloride, 5 mM magnesium acetate, 1 mM DTT, 0.025% Triton X-100, and protease inhibitors). Sepharose beads were washed three times in IPP buffer, and precipitated material was resuspended in TRIzol reagent (Invitrogen). Associated RNA was isolated and reverse transcribed, and PCR analysis was performed as described above.

CsA application in vivo

Animals were held in cages with constant temperature and humidity and drinking water and food ad libitum. The local review board approved this animal experiment according to prevailing guidelines for scientific animal experimentation. Male and female 14–16-wk-old C57BL/6 mice (The Jackson Laboratory, Bar Harbor, ME) with a weight of 20 g received a single dose of CsA, dissolved in olive oil, by s.c. injection at a concentration of 100 mg/kg body weight (n = 4, one male and three females). Control animals received s.c. injections of olive oil only (n = 3, one male and two females). Ten hours after injection, animals were sacrificed, and kidneys were removed and frozen on dry ice for protein extraction or immunofluorescence. Extraction of proteins from renal cortical tissues was performed as described before (23).

Immunofluorescence

Immunofluorescence was performed on 4-μm cryosections fixed in −20°C acetone and washed twice in PBS. Sections were incubated with a primary Ab specific for YB-1 (polyclonal Ab against protein C terminus; from http://www.antibodies-online.com) for 1 h at RT. Sections were washed three times in PBS and incubated with the secondary Ab Alexa Fluor 488-conjugated goat anti-rabbit IgG (MoBiTech) for 30 min. After washing twice with PBS, coverslips were mounted on glass slides with Immu-Mount (Thermo Fisher Scientific), and images were taken with an Olympus BX50 (Color View, Soft Imaging System; software: analySIS Pro).

Statistical analysis

All values are expressed as the means ± SD. Statistical significance was evaluated using the Student t test with significance accepted when $p < 0.05$. All in vitro experiments were performed at least in triplicate.

Results

CsA influences YB-1 content in kidney cells

To investigate the impact of YB-1 during CNI-triggered kidney fibrosis, we analyzed different renal cells regarding their YB-1 expression upon challenge with CsA. For this, rMCs, hMCs, HK-2, and HEK293T cells, as well as undifferentiated mouse podocytes (WT5), were incubated for 4 h with CsA using a therapeutically relevant dose of 1 μM. As a control, cells were incubated for equal times with the solvent DMSO only. CsA treatment resulted in a robust increase of intracellular YB-1 protein amounts in rMCs and hMCs (Fig. 1*A*, *upper panel*). In contrast, HK-2 and WT5 cells (Fig. 1*A*, *lower panel*) showed a decreased YB-1 protein amount upon CsA treatment. Intracellular YB-1 protein content in HEK293T cells was not altered following CsA incubation (Fig. 1*A*, *lower panel*).

Next, we extended our studies to another CNI, namely Tac, and to the mammalian target of rapamycin inhibitor rapamycin. A comparable stimulatory effect on YB-1 expression was found for Tac (Fig. 1*B*). However, rapamycin displayed no efficiency to enhance the intracellular YB-1 protein amount in rMCs (Fig. 1*C*).

CNIs induce a rapid and dose-dependent elevation of YB-1 protein content in MCs

To investigate the dose and time dependency of the CNI effects on YB-1 expression, we opted for rMCs for the subsequent

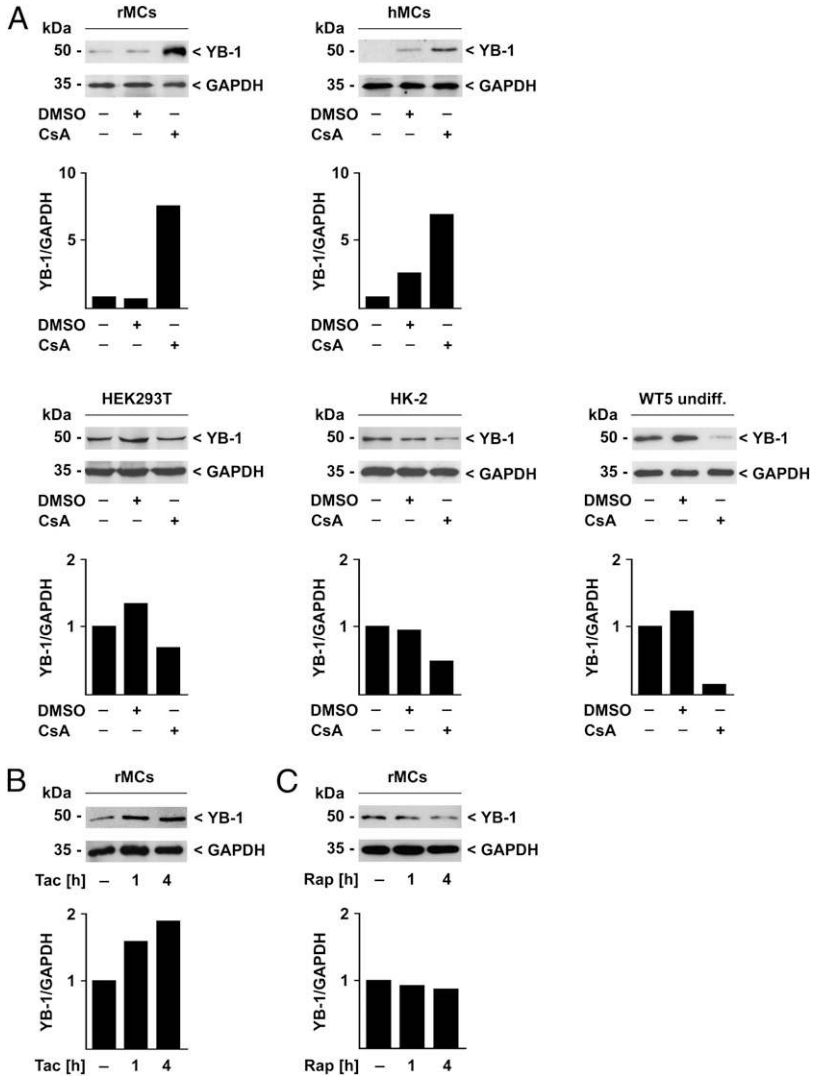

FIGURE 1. *A*, Influence of CsA on YB-1 protein content is cell specific. Different renal cells were treated with CsA (1 μM) or vehicle for 4 h, and YB-1 protein expression was determined by immunoblot analysis using a polyclonal anti–YB-1 Ab raised against the C terminus. Densitometry of bands was performed with normalization against GAPDH. Relative band intensities are depicted in the histogram below. rMCs were incubated for 1 or 4 h with Tac (0.01 μM; *B*) or rapamycin (0.05 μM; *C*), and YB-1 protein content monitored by Western blot was compared with vehicle (DMSO)-treated cells. rMCs, hMCs, HEK293T cells, human renal proximal tubular cells (HK-2), immortalized undifferentiated podocytes (WT5). Representative results of three independent experiments are shown.

experiments because these cells displayed the highest increase of YB-1 protein content upon CsA treatment (Fig. 1). Furthermore, MCs are of particular importance in glomerular fibrogenesis as they are important producers of ECM components. The time course of YB-1 upregulation upon CsA incubation was investigated in more detail. Within 1 h, a 9-fold increase of YB-1 protein content was detected that lasted for 4 h and gradually declined after 8 h of CsA challenge (Fig. 2*A*). Tac led to a similar >5-fold augmented YB-1 protein content in comparison with vehicle (DMSO)-treated cells, and a markedly elevated amount persisted over a 24-h period (Fig. 2*B*). In contrast, the level of GAPDH remained unchanged upon inhibition, indicating that the marked YB-1 increase is due to a specific process but not to an overall protein accumulation.

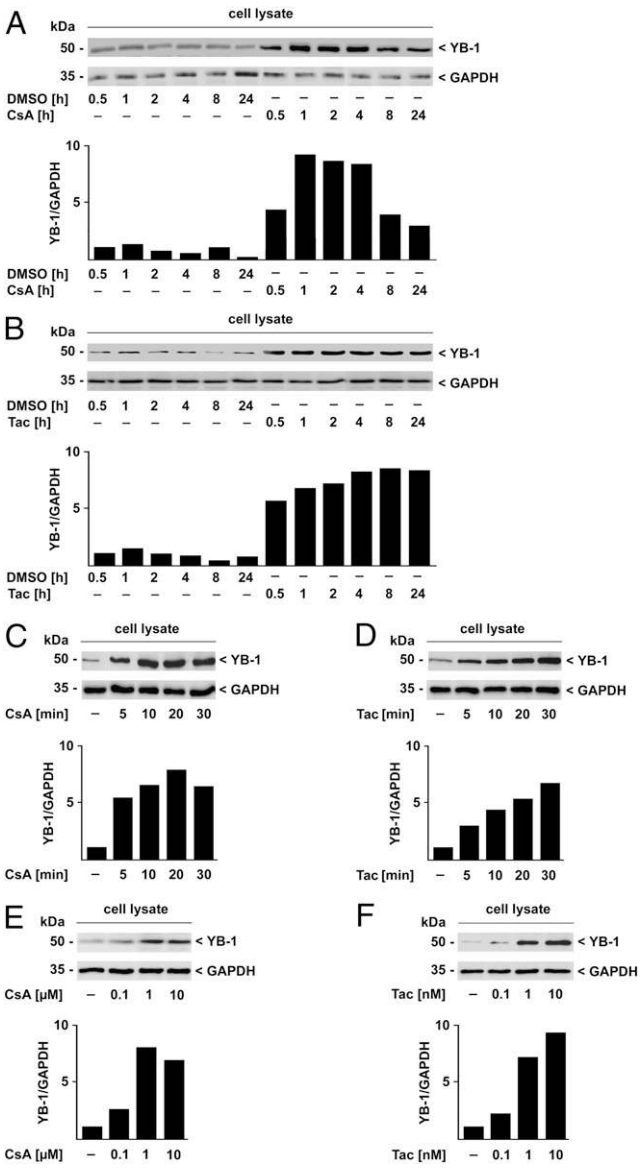

FIGURE 2. CNI-dependent YB-1 upregulation is time and dose dependent. rMCs were incubated for the indicated long or short time periods with CsA (1 μM; *A*, *C*) or Tac (0.01 μM; *B*, *D*) and YB-1 content was visualized by Western blot analysis. Dose-dependency was investigated by using increasing concentrations of CsA (*E*) and Tac (*F*) to stimulate rMCs. Loading of equal protein amounts was ascertained by incubating all blots with GAPDH. Relative band intensities are depicted in the histogram below. Representative results of three independent experiments are shown.

Because the CNI-induced increase of YB-1 protein was observed already 30 min after CsA and Tac exposure, we next performed a short-term kinetic for both CNIs starting at 5 min. As can be seen in Fig. 2*C* and 2*D*, intracellular YB-1 protein content more than doubled as early as 5 min after CNI administration.

Next, the dose-response dependency of CsA/Tac challenge and intracellular YB-1 content was analyzed, considering the respective concentration range encompassing therapeutically relevant doses. As can be seen in Fig. 2*E*, incremental CsA doses from 0.01–1 μM induced a dose-dependent YB-1 protein increase, whereas a further elevation to 10 μM did not result in an additional escalation. A comparable dose dependency was obtained with Tac, whereby a concentration as low as 10 nM was sufficient for maximal cellular response (Fig. 1*E*), reflecting its higher pharmacological potency to inhibit calcineurin (31).

Taken together, CNIs CsA and Tac induce an extremely rapid and dose-dependent increase of YB-1 content in a cell type-specific manner.

Augmented YB-1 expression is due to translation and enhanced protein stability rather than to a transcriptional process

To define more precisely the cellular mechanism of the very rapid enhancement of YB-1 expression in rMCs upon CNI administration, we evaluated the YB-1 mRNA content in rMCs after administration of CsA. CNI application for up to 24 h did not significantly increase YB-1 transcript levels in comparison with vehicle-treated cells investigated by qRT-PCR (data not shown). To support the idea that gene expression is not the major cause for the immediate YB-1 increase, we included specific inhibitors of transcription, Act.D (Fig. 3*A*, *lanes 3* and *5*), and of translation, CHX (Fig. 3*A*, *lanes 4* and *6*), in the CsA incubation assays. Cells incubated solely with DMSO (*lane 1*) or CsA (*lane 2*) for 4 h served as negative and positive controls, respectively. Although both inhibitors were found to block the CsA-induced YB-1 upregulation, the inhibitory effect was substantially higher by hindering the translational machinery (Fig. 3*A*, *lane 5* compared with *lane 6*). However, blocking of translation had no effect on the early accumulation of YB-1 protein (Fig. 3*B*, *lane 2*).

To evaluate the contribution of protein stability on the elevated YB-1 content, we next assessed the influence of the cell-permeable proteasome inhibitor MG132, because a 20S proteasome-mediated cleavage of YB-1 at glycine 220 has been described (32). To prove the hypothesis that hindered degradation of YB-1 can induce a conspicuous protein elevation, rMCs were challenged with two different concentrations (10 and 50 μM) of MG132 either in the presence or absence of CsA, respectively. In comparison with untreated cells (Fig. 3*C*, *lane 1*), application of MG132 at a concentration of 10 μM resulted in a 3-fold induction of YB-1 protein content and ~8-fold when 50 μM was applied (Fig. 3*C*, *lanes 2* and *3*). GAPDH levels remained unchanged at both concentrations. This specific increase of YB-1 protein content as a consequence of proteasome inhibition was comparable to the one achieved by CsA administration (Fig. 3*C*, *lane 4*); however, combined incubation of CsA and MG132 did not lead to a YB-1 increase beyond the one observed with either component alone (Fig. 3*C*, *lanes 5* and *6*).

To narrow down the time slot of YB-1 degradation, rMCs were treated with CHX either after preincubation for 8 h with CsA or solely exposed to CHX for different time periods. In the case of suppressed translation, the protein content of YB-1 in control cells declined steadily starting immediately after CHX incubation (Fig. 3*D*, *lanes 2–6*). In contrast, rMCs that exhibited an elevated YB-1 content due to preincubation with CsA still contained >60% of the initial YB-1 protein amount 8 h after CHX treatment was

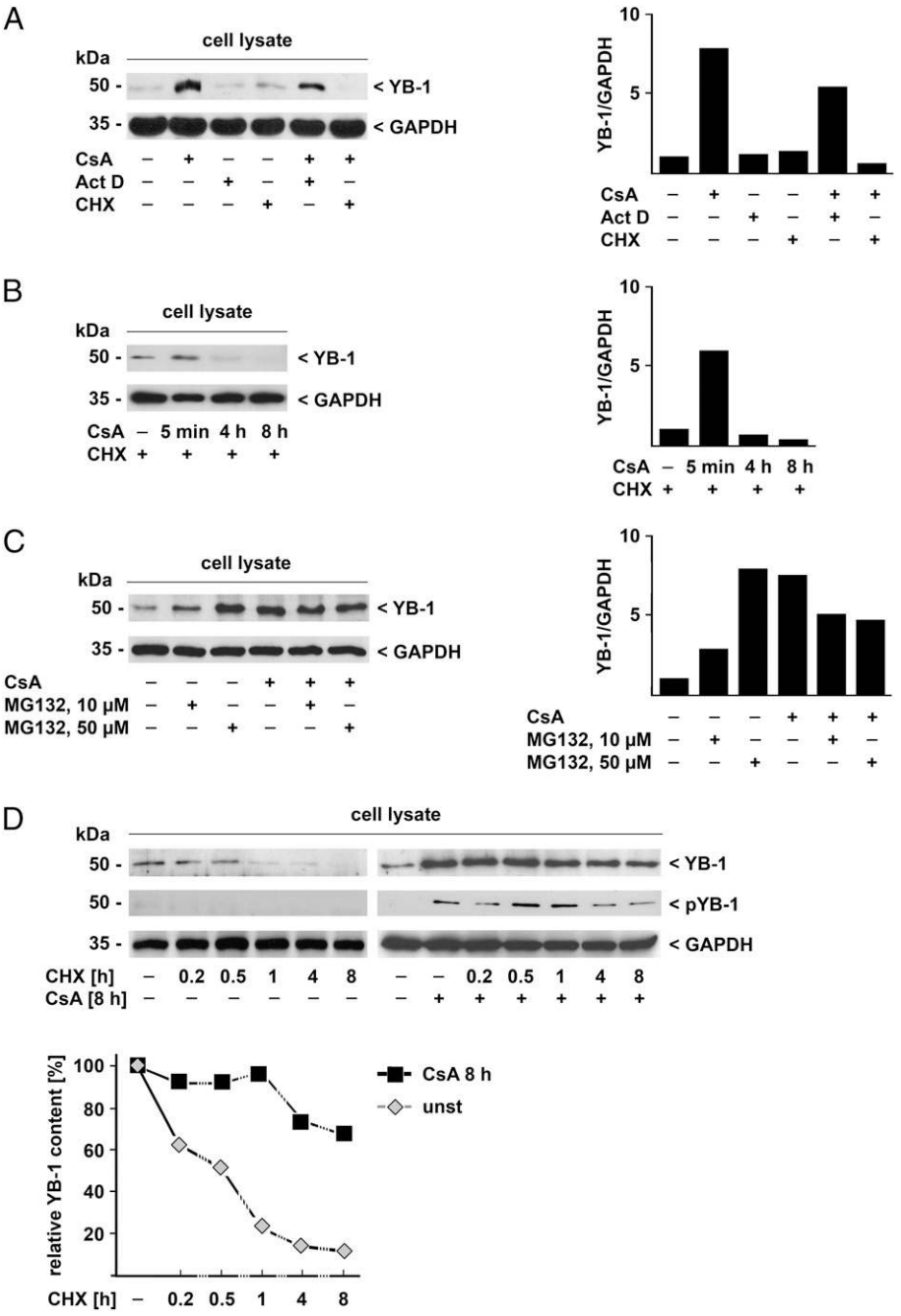

FIGURE 3. Posttranscriptional regulation of YB-1 expression in rMCs upon CsA application. *A*, Prior to DMSO (as vehicle) or CsA application (4 h), a 15 min-preincubation step either with Act.D (10 μM) as a specific inhibitor for transcription or alternatively with CHX (10 μM) to prevent translation was performed. For Western blot analysis, cell protein extracts were subjected to SDS-PAGE and probed with a polyclonal anti–YB-1 Ab and anti-GAPDH as loading control. *B*, Subsequent to CHX incubation (10 μM), CsA was applied for the indicated times, and YB-1 was detected. *C*, MCs were treated with proteasome inhibitor MG132 at two different concentrations together or without CsA. Densitometry of bands was performed with normalization against GAPDH. Relative band intensities are depicted in the histogram below. *D*, YB-1 protein stability and phosphorylation was investigated under conditions of disabled translation in the presence of CHX (10 μM) with or without CsA incubation. Densitometry of bands was performed with normalization against GAPDH. Relative band intensities throughout the time periods are depicted in the graph whereby in each assay, bands corresponding to the cells without CHX inclusion were set to 100%. Shown is one experiment representative for three independent experiments with similar results.

started (Fig. 3*D*, *lanes 8–13*). Following challenge with CsA, a marked phosphorylation of YB-1 protein was observed that persisted over the observed period of time (Fig. 3*D*, *middle panel*).

Thus, the rapid and profound increase of intracellular YB-1 protein content following CsA treatment relates to posttranscriptional mechanisms such as enhanced translation and decreased protein degradation.

ROS are involved in the CsA-triggered YB-1 protein increase, independent of TGF-β

Because CsA triggers the generation of ROS (33), we investigated whether the CNI-induced upregulation of YB-1 is dependent on ROS production. Again, rMCs were stimulated with CsA, but this time, the cells were preincubated for 30 min with different inhibitors of redox signaling cascade, namely Nac and DPI.

Whereas the amount of CsA-dependent increase of YB-1 protein content was entirely abolished by preincubation with the antioxidant Nac (Fig. 4*A*, *lane* 3), an inhibitor of flavin-containing enzymes (NADPH oxidases), DPI, prompted a moderate inhibition (Fig. 4A, *lane 4*). To assess the molecular source of CsA-triggered ROS generation, we introduced specific scavengers and ROS-converting enzymes, namely peroxynitrite scavenger Ebs, PEG-SOD, and Cat. The HXXO that generates an extracellular flux of superoxide anion radical ($O_2^{\cdot -}$) and H_2O_2 served as positive control (*lane 8*). Among the used ROS scavengers, Cat was the most potent one to inhibit the CsA-induced effect (Fig. 4*A*, *lane 7*). Because Cat accounts for decomposition of H_2O_2, our results indicated that H_2O_2 rather than superoxide was responsible for CsA-triggered YB-1 elevation in rMCs. To prove a direct influence of H_2O_2 on YB-1 expression, we incubated rMCs for either 10 min or 4 h with H_2O_2 at different concentrations starting at 10 μM. In full accordance with ROS scavenger experiments, an increase of YB-1 protein content was observed already 10 min after H_2O_2 exposure (Fig. 4*B*, *lanes 2–4*), and this occurred in

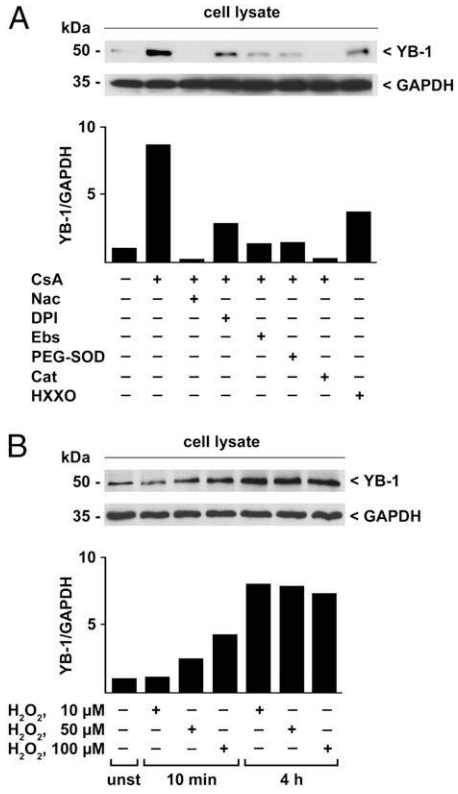

FIGURE 4. ROS are involved in CsA-triggered YB-1 protein increase. *A*, Prior to CsA challenge (1 μM), rMCs were preincubated with different inhibitors of redox signaling cascade, namely Nac and DPI and different ROS scavengers such as Ebs (10 μM), PEG-SOD (100 U/ml), and Cat (500 U/ml) for 30 min before intracellular YB-1 content was assessed by Western blot analyses. The HXXO (8 U/ml, 50 μM) served as positive control. *B*, rMCs were incubated either for 10 min or 4 h with H_2O_2 at different concentrations or with vehicle DMSO. Representative results of three independent experiments are shown.

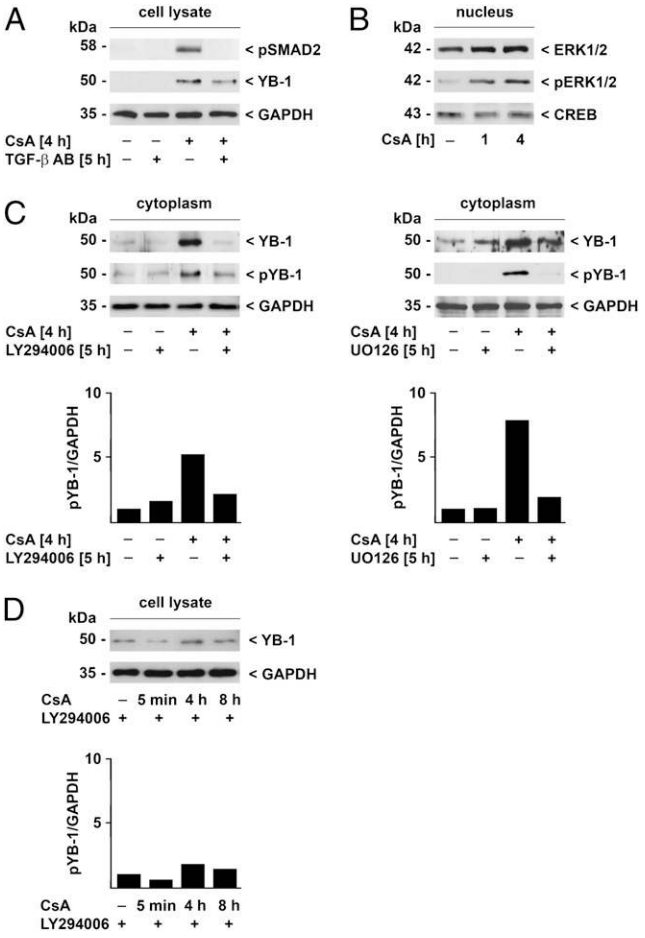

FIGURE 5. CNI-induced YB-1 protein increase is independent from TGF-β but involves the ERK/AKT phosphorylation pathway. *A*, To neutralize TGF-β, rMCs were incubated with an inhibitory anti–TGF-β Ab 1 h prior to CsA stimulation (1 μM). YB-1 content and phosphorylation of SMAD2 was assessed by Western blot analyses using GAPDH as loading control. *B*, Total ERK1 and phospho-ERK1 was monitored in nuclear protein extracts of rMCs stimulated for 1 or 4 h with CsA (1 μM) and compared with cells left untreated. Equal protein loading was ensured by determining CREB levels using anti-CREB Abs. *C*, rMCs were preincubated with specific inhibitors for Akt (LY294006; 10 μM), ERK (UO126; 10 μM) kinases or solvent 1 h prior to CsA challenge (1 μM) or left untreated. Total cell protein extracts were probed for nonphosphorylated as well as for phosphorylated YB-1 using specific anti–YB-1 Abs. GAPDH served as loading control. *D*, rMCs were preincubated with specific inhibitors for Akt (LY294006; 10 μM), and YB-1 protein content was detected after CsA was applied for the indicated times. Representative results of three independent experiments are shown.

a dose-dependent manner peaking in a 4-fold induction of YB-1 protein content at 100 μM H_2O_2. Prolonged incubation time (4 h) resulted in a >6-fold upregulation of YB-1 without a dose-dependent effect (Fig. 4*B*, *lanes 5–7*). These data strongly suggest that the CNI-triggered increase of cellular YB-1 content is mediated by generation of H_2O_2.

TGF-β has been described to be a central mediator of CNI-induced renal fibrogenesis, and the phosphorylation of SMAD2 is a key feature of downstream TGF-β signaling pathway. In our experiments, the neutralization of TGF-β using an inhibiting Ab abolished the CNI-induced SMAD2 phosphorylation (Fig. 5*A*, *upper panel*, *lane 4*) following CsA exposure (Fig. 5*A*, *upper panel*, *lane 3*). However, the CsA-induced YB-1 increase was similar in cells treated with nonspecific IgG or anti-TGF-β Ab (Fig. 5*A*, *middle panel*, *lanes 3* and *4*). Thus, the inhibition of the TGF-β pathway did not influence the CsA-induced increase of YB-1 expression.

The YB-1 phosphorylation status is altered in response to CsA

Given the fact that YB-1 is a downstream target of MAPK ERK1/2 (34, 35), we analyzed the involvement of ERK1/2 in CsA-triggered cell activation. Following treatment of rMCs with CsA for either 1 or 4 h, we observed an increase of phosphorylated ERK1/2$^{T202/Y204}$ in the nucleus at both time points, whereas CREB and total ERK1/2 levels remained constant (Fig. 5*B*).

It is well documented that YB-1 undergoes phosphorylation at serine 102 (Ser^{102}) by activated serine/threonine protein kinase Akt/protein kinase B (36, 37). To analyze whether the CNI-triggered YB-1 increase is dependent on phosphorylation, as this was shown following application of CsA to rMCs (Fig. 3*D*, *middle panel*), we introduced a specific pharmacological Akt inhibitor (LY294006) and analyzed the YB-1 content/phosphorylation status following CsA challenge of rMCs. Akt inhibition completely abolished CsA-induced YB-1 increase (Fig. 5*C*, *left upper panel*). Furthermore, 4 h after CsA challenge, a marked phosphorylation at Ser^{102} within the YB-1 protein was observed (Fig. 5*C*, *left middle panel*, *lane 3*) that was absent after preincubation with Akt kinase inhibitor (Fig. 5*C*, *left middle panel*, *lane 4*). When ERK phosphorylation was prevented by UO126 application, the inhibitory effect was similarly profound (Fig. 5*C*, *right middle panel*, *lane 4*). Equally to the effects observed after 4 h, Akt kinase

inhibition entirely prevented the increase of YB-1 protein that normally occurs within minutes (Fig. 5*D*).

Thus, inhibition of Akt/ERK signals upstream of YB-1 activation prevents its phosphorylation at Ser^{102} and abolishes the CsA-mediated YB-1 protein increase.

YB-1–mediated collagen increase in rMCs upon CsA challenge

Next, we examined fibrogenic responses in rMCs. By performing quantitative real-time PCR and protein quantification, we examined the expression of Col1A after CsA treatment in rMCs with regular YB-1 expression and compared this to YB-1 knockdown cells (Fig. 6*A*, *lanes 2* and *3*). Col1A mRNA significantly increased 1 h following CsA application in comparison with control cells and then tapered off (Fig. 6*B*, light gray columns). Furthermore, there was a raised collagen protein content in CsA-treated cells (data not shown). Knockdown of endogenous YB-1 resulted in a significantly lower increase of collagen mRNA level after CsA application (Fig. 6*B*, dark gray and black columns).

Because YB-1 serves as a negative regulator of Col1A gene transcription by binding to a proximal Y-box element within the Col1A promoter, we speculated that enhanced protein synthesis upon CsA-induced YB-1 increase was rather due to higher mRNA stability, as reported, for example, for the vascular endothelial growth factor (38). Therefore, we analyzed the collagen mRNA content following CsA treatment, but under conditions of hindered gene transcription. As can be seen in Fig. 6*C*, CsA incubation markedly prolonged the $t_{1/2}$ of YB-1 and collagen transcripts in rMCs. Compared to CsA-treated cells, a decrease of YB-1 mRNA in cells without prior CsA challenge occurred during 30 min of Act.D incubation. These results were confirmed by qRT-PCR that demonstrated a 50% reduction of collagen mRNA content within 1 h when subsequent delivery of transcripts was prevented by Act. D (Fig. 6*D*). In contrast to this, under conditions of CsA treatment, Col1A mRNA content was unchanged 1 h posttreatment. Thus, CNI application results in strikingly increased collagen mRNA stability.

Next, we analyzed whether a physical interaction of YB-1 with collagen mRNA after CsA application occurs and whether this is responsible for the enhanced mRNA stability. For this, YB-1 was immunoprecipitated from cytoplasmic rMC extracts with and without prior CsA challenge. Coprecipitated mRNA was isolated and detected by RT-PCR (Fig. 6*E*). In comparison with unstimulated cells, a 2-fold increase in YB-1–mRNA (Fig. 6*E*, *left upper panel*, *lane 4*) and 4-fold more ColA transcripts bound to YB-1 were precipitated from cells prior stimulated with CsA (Fig. 6*E*, *left middle panel*, *lane 4*).

CsA influences YB-1 content in renal cells in vivo

To verify our in vitro results in vivo, we injected mice s.c. with CsA or vehicle (olive oil) and analyzed renal YB-1 content 8 h after

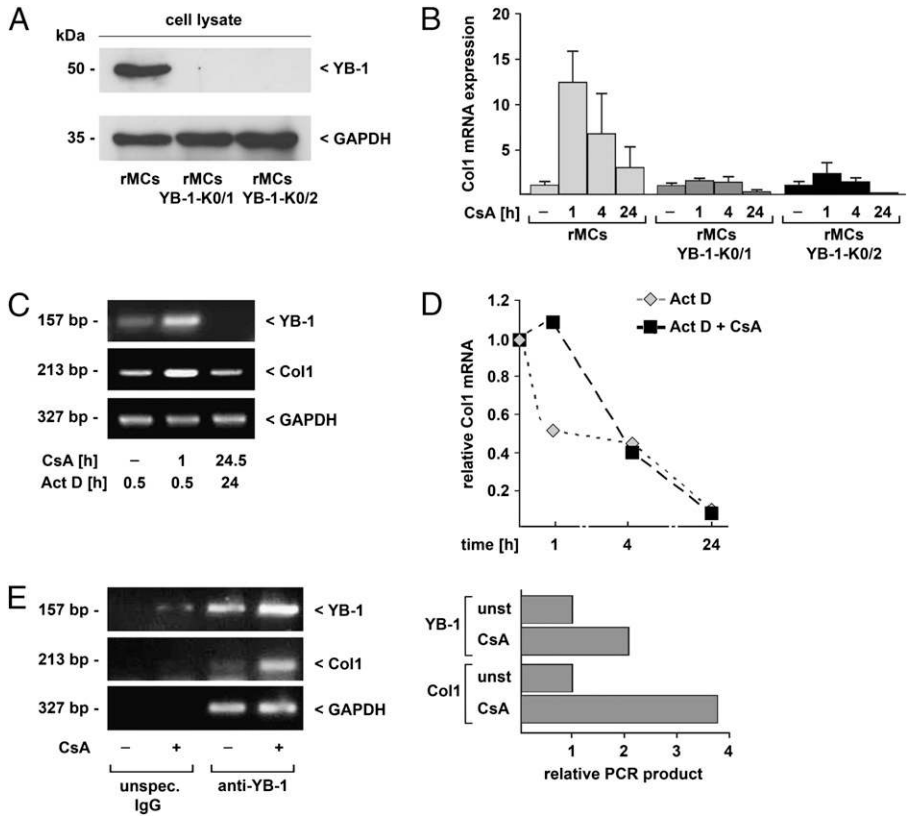

FIGURE 6. Enhanced expression of collagen 1 upon CsA incubation in rMCs is dependent on YB-1, whereas YB-1 directly binds and thereby stabilizes collagen 1 and YB-1 mRNA. *A*, Comparison of YB-1 expression in rMCs to that of YB-1 knockdown cells by Western blot technique. A total of 20 μg total protein cell extract was analyzed for YB-1 expression using a C-terminal anti–YB-1 and anti-GAPH Ab as loading control, respectively. *B*, Collagen 1 transcript numbers were quantified in rMCs and in two clones of YB-1 knockdown cells at different time points following CsA incubation. By quantitative TaqMan analysis, mRNA was normalized for the 18S RNA content, whereby value of unstimulated rMCs was set as 1. Values are means ± SD ($n = 3$). Collagen 1 mRNA stability with and without CsA challenge was analyzed by RT-PCR (*C*) at different time points under conditions of hindered gene transcription by inclusion of Act.D (10 μM) and quantified by TaqMan analysis (*D*). *E*, Physical interaction of YB-1 with YB-1 and collagen mRNA was analyzed in cytoplasmic rMC extracts with and without prior CsA challenge by immunoprecipitation using anti–YB-1 Ab and unspecific IgG as control. Coimmunoprecipitated mRNA was isolated, reverse transcribed, and detected by RT-PCR. PCR products were quantified, whereby values of unstimulated rMCs were set as 1. Representative results of three independent experiments are shown.

injection. Immunoblotting of total kidney protein extracts revealed an elevated YB-1 protein content in the group of CsA-treated mice in comparison with control animals (Fig. 7*A*). The GAPDH content remained unchanged upon CsA application, indicating that the YB-1 increase is due to a specific process but not to an overall protein accumulation. To localize more specifically the enhanced YB-1 expression in the kidney, we performed immunofluorescence with a polyclonal anti–YB-1 Ab. In animals with CsA application, increased YB-1 staining was detected in the mesangial compartment in comparison with olive oil-injected mice (Fig. 7*B*).

Discussion

Clinical use of the calcineurin inhibitors CsA and Tac is limited by their various side effects (e.g., nephrotoxicity), and CNIs may mediate excessive accumulation and deposition of ECM and thereby harm the renal allograft (39). Activation of matrix-producing effector cells such as glomerular MCs, interstitial fibroblasts, and tubular epithelial cells is a central event in renal fibrogenesis (40, 41). As a model for CNI-mediated glomerular effects, we focused on MCs because these cells are critically involved in the progression of renal fibrosis.

Hallmarks of mesangial activation during fibrogenesis are de novo expression of α-smooth muscle actin and overproduction of interstitial matrix components such as Col1A. YB-1 has been demonstrated to serve as a potent negative transcriptional regulator of both genes (19, 26, 28, 29), whereas it *trans*-activates expression of MMP-2, a matrix-degrading enzyme (20, 42). These findings, together with the fact that YB-1 interferes with the signaling pathway of the central fibrotic factor TGF-β (43), have led to the assumption that YB-1 represents an antifibrotic factor. Opposing functions of YB-1 on both transcription and translation may explain the controversial results on Col1A generation in CsA-induced nephropathy described in this study compared with previous observations. YB-1 negatively regulates Col1A gene transcription by binding to a proximal Y-box element, which is highly conserved among humans, rats, and mice (19). However, the strong increase of YB-1 protein content in MCs upon CsA treatment directly correlates with an enhanced rate of collagen message and protein, as CsA-triggered Col1A expression is prevented in YB-1 knockdown cells.

In contrast to MCs, renal tubular epithelial (HK-2) and podocyte precursor cells exhibited a decreased intracellular YB-1 protein content following CsA incubation (Fig. 1*A*, *bottom panel*). Because YB-1 is important in preventing premature senescence, which has been demonstrated in YB-1 knockdown mice (44), a diminished YB-1 content may cause an impaired proliferation. This is in line with the observations in renal tubular epithelial cells, in which CsA mediates cell cycle arrest (45) and enhanced senescence (46), potentially mediated by YB-1 depletion.

The evolutionarily highly conserved Y-box proteins are important components of the eukaryotic redox signaling pathway (47), and in line with this, embryonic fibroblasts from YB-$1^{d/d}$ mice exhibit a reduced ability to respond to oxidative-induced stress (15). In search of the mechanisms of CsA-dependent YB-1 upregulation, we identified H_2O_2 to be involved in this pathway. H_2O_2 led to a significant induction of YB-1 protein content in rMCs to a comparable degree as that observed after CsA treatment, and specific interference in H_2O_2 generation/persistence by either DPI or Cat resulted in a blockade of YB-1 upregulation. Of note, the addition of exogenous ROS (48) to MCs upregulates gene expression of RANTES, another well-described target YB-1 gene (21, 22). Recent data provide evidence for the impact of ROS on latent TGF-β activation in rMCs (14). However, in contrast to YB-1 upregulation, superoxide, but not H_2O_2, is responsible for CNI-induced TGF-β–dependent SMAD signaling. Together with our observation that an inhibition of the TGF-β pathway does not affect YB-1 protein increase, YB-1 appears to be a TGF-β–independent downstream target of CsA. Thus, YB-1 might be another important profibrotic factor induced by CsA, perhaps upstream but at least in a TGF-β–independent manner. Of note, YB-1 controls TGF-β translation in proximal tubular cells (17).

The rapid YB-1 induction in renal cells by CsA and Tac within minutes resembles the fast, CNI-triggered induction of the latent form of TGF-β (14). Because CNI-dependent YB-1 upregulation is comparably fast and equally independent of de novo gene transcription (Fig. 3*A*), we proposed posttranscriptional mechanisms to account for YB-1 maintenance/generation. This

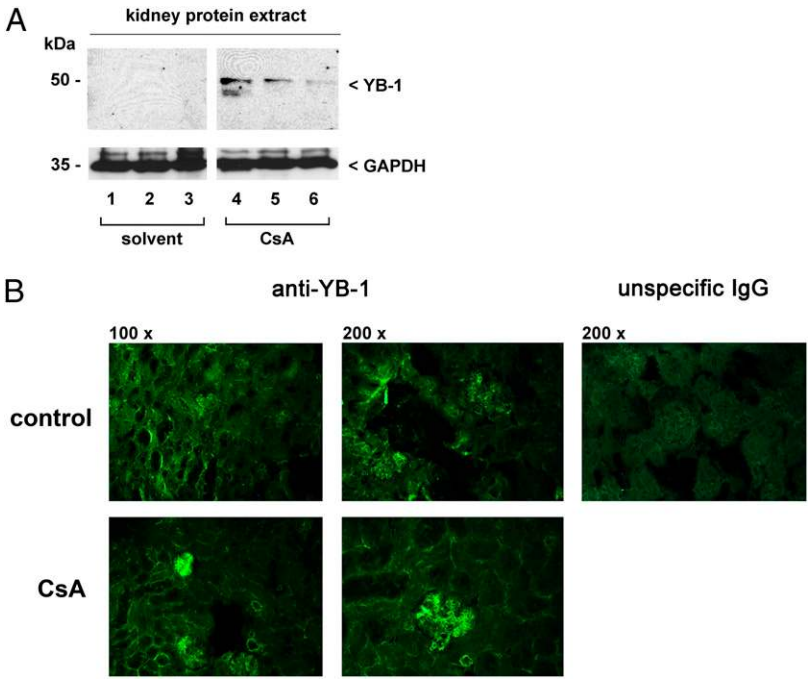

FIGURE 7. CsA influences YB-1 content in renal cells in vivo. *A*, Immunoblotting of total kidney protein extracts from mice 8 h after injection of CsA (100 mg/kg body weight) in comparison with olive oil-injected animals as control. YB-1 content was assessed by Western blot analyses using polyclonal anti–YB-1 Ab raised against the C terminus. GAPDH amount served as loading control. *B*, YB-1 expression in kidney specimen of animals without and subsequent to CsA stimulation (8 h) was visualized by fluorescence microscopy using anti–YB-1 Ab and Alexa Fluor 488-conjugated secondary Ab (green). Original magnification ×100 (*left panels*) and ×200 (*middle* and *right panels*).

assumption is corroborated by our experiments with translational inhibitor CHX that is able to effectively block the CNI-initiated YB-1 increase in rMCs in contrast to hindered transcription. In contrast, YB-1 protein stability is strikingly enhanced in the presence of CsA (Fig. 3*D*), suggesting that the observed early increases in YB-1 expression are caused by hindered degradation. Of note, blocking of translation had no effect on the early accumulation of YB-1 protein. Furthermore, the proteasome inhibitor MG132 significantly elevated YB-1 protein content. Similarly, H_2O_2 prevents proteasomal degradation of the transcription factor c-*fos* in cardiomyocytes through phosphorylation (49). In podocytes, CsA treatment efficiently blocks protein degradation of synaptopodin (50). Conceivably, impaired YB-1 protein degradation, which is the consequence of enhanced protein stability or a possible saturation of the degradation process, may explain the immediate YB-1 accumulation that occurs within only minutes after CsA application to rMCs.

The high protein content of YB-1 is maintained by augmented translation. In higher eukaryotes, a large proportion of mRNA species is preferentially localized to nonpolysomal fractions in translationally inactive mRNA particles (mRNPs), and YB-1 serves as a universal protein of cytoplasm mRNPs (51). Under conditions of serum starvation or stress, the population of nonpolysomal mRNPs is increased, whereas YB-1–associated messages encode stress- and growth-related proteins (37). Because YB-1 acts as a cap-dependent mRNA stabilizer (52), the increase of YB-1 protein in rMCs upon CsA application may result in enhanced mRNA–YB-1 interaction and stabilization of different proteins (e.g., of Col1A). Indeed, we observed a CsA-dependent increase in Col1A mRNA stability independent of preceding gene transcription and an enhanced physical interaction between YB-1 and Col1A mRNA following CsA treatment. Therefore, YB-1 maintains a backup pool of various mRNAs, including its own, that enables rapid access for protein synthesis avoiding prior gene promoter activation.

In addition to mRNA stabilization, YB-1 actively controls RNA translation, either in an activating (53) or repressive (36) manner. Notably, YB-1 regulates translation of its own mRNA (32, 51). As an inhibitor of translation, YB-1 binds to the capped 5′ terminus of mRNAs encoding proteins that are associated with cell growth and oncogenesis to inhibit their translation (54). In response to extracellular stimuli, the phosphorylation status of YB-1 is altered, and as the phosphorylated form of YB-1 possesses a lower affinity for the cap structure of mRNA, YB-1 dissociates from mRNA (36). In our study, we demonstrated that CsA-induced YB-1 accumulation was dependent on MAPK/ERK and PI3K/Akt pathways, as specific kinase inhibitors counteract CsA-initiated effects on YB-1 (Fig. 5). YB-1 phosphorylation by these pathways is already well documented. Because the inhibition of Akt kinase completely abolished the CsA-induced YB-1 increase that occurs within minutes as well as the increase after 4 h, we propose that both mechanisms, the enhanced protein stability and mRNA-stability/translation, are enabled by prior phosphorylation of YB-1. A phosphorylation-triggered release of YB-1 from mRNA may result in an induced collagen protein synthesis. Of note, TGF-β also activates MAPK, with ERK enhancing the TGF-β–stimulated Col1A synthesis (55).

We assume that a sequence of consecutive biochemical processes is responsible for the very strong increase of YB-1 protein in MCs in response to CNI treatment with phosphorylation obviously being a key event (Fig. 8). In this study, we elucidate the underlying mechanisms of CNI-mediated YB-1 protein increase that encompasses phosphorylation of YB-1 by Akt and ERK pathways and demonstrate that the efficacy of YB-1 translation and subsequently of collagen is controlled by a markedly prolonged $t_{1/2}$ of mRNA in rMCs.

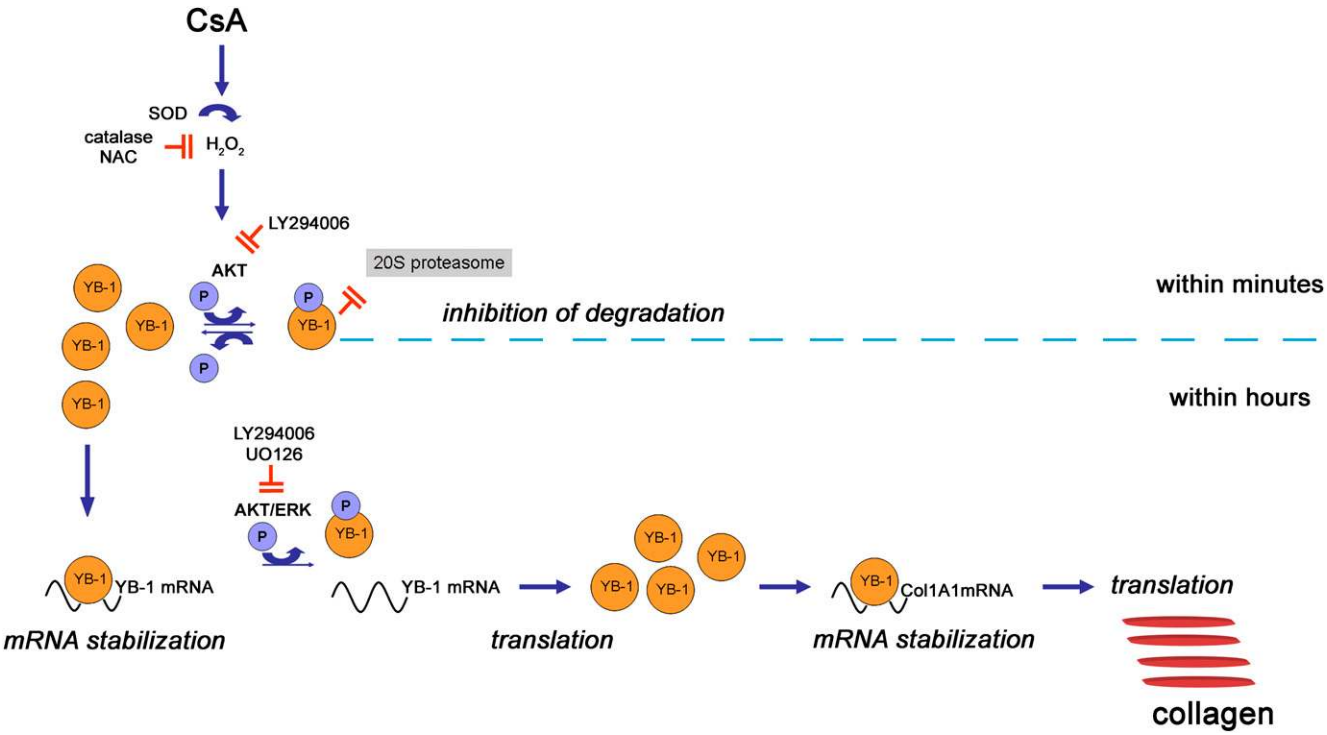

FIGURE 8. Schematic model of YB-1 governing collagen synthesis upon CsA response in mesangial cells. CsA induces H_2O_2-triggered increase on YB-1 content by protein and mRNA stabilization that involves AKT/ERK kinase pathways. Direct physical interaction of YB-1 with collagen mRNA stabilizes transcripts and promotes collagen synthesis in MCs.

Our data assign another important role to YB-1 in the context of kidney transplantation. Recent data from our group already identified YB-1 as a cell type-specific regulator of one of the key mediators exhibiting chemotactic potential in kidney transplant rejection, namely the C-C chemokine RANTES/CCL5. Through regulation of differential expression in infiltrating monocytes, macrophages, and T cells, YB-1 potentially acts as an adaptive controller of inflammation under conditions of kidney allograft rejection (21). In this study, we report that CNI-mediated fibrosis may be partially explained by augmented YB-1 protein maintenance/expression in MCs that we could demonstrate in vitro and in vivo. Of special interest is the fact that rapamycin, an immunosuppressive drug with reduced, or even without, fibrogenic potential (56), does not affect YB-1 content in MCs (Fig. 1*C*).

Acknowledgments

We thank Monika Cordes and Marina Wolf El-Houari for technical assistance and the group of Ostareck-Lederer/Ostareck for help with coimmunoprecipitation of mRNA.

Disclosures

The authors have no financial conflicts of interest.

References

1. Burke, J. F., Jr., J. D. Pirsch, E. L. Ramos, D. R. Salomon, D. M. Stablein, D. H. Van Buren, and J. C. West. 1994. Long-term efficacy and safety of cyclosporine in renal-transplant recipients. *N. Engl. J. Med.* 331: 358–363.
2. Hariharan, S., C. P. Johnson, B. A. Bresnahan, S. E. Taranto, M. J. McIntosh, and D. Stablein. 2000. Improved graft survival after renal transplantation in the United States, 1988 to 1996. *N. Engl. J. Med.* 342: 605–612.
3. Tilney, N. L., E. L. Milford, J. L. Araujo, T. B. Strom, C. B. Carpenter, and R. L. Kirkman. 1984. Experience with cyclosporine and steroids in clinical renal transplantation. *Ann. Surg.* 200: 605–613.
4. Mihatsch, M. J., M. Kyo, K. Morozumi, Y. Yamaguchi, V. Nickeleit, and B. Ryffel. 1998. The side-effects of ciclosporine-A and tacrolimus. *Clin. Nephrol.* 49: 356–363.
5. Ekberg, H. 2008. Calcineurin inhibitor sparing in renal transplantation. *Transplantation* 86: 761–767.
6. Ninova, D., M. Covarrubias, D. J. Rea, W. D. Park, J. P. Grande, and M. D. Stegall. 2004. Acute nephrotoxicity of tacrolimus and sirolimus in renal isografts: differential intragraft expression of transforming growth factor-beta1 and alpha-smooth muscle actin. *Transplantation* 78: 338–344.
7. Shihab, F. S., T. F. Andoh, A. M. Tanner, and W. M. Bennett. 1997. Sodium depletion enhances fibrosis and the expression of TGF-beta1 and matrix proteins in experimental chronic cyclosporine nephropathy. *Am. J. Kidney Dis.* 30: 71–81.
8. Ignotz, R. A., and J. Massagué. 1986. Transforming growth factor-beta stimulates the expression of fibronectin and collagen and their incorporation into the extracellular matrix. *J. Biol. Chem.* 261: 4337–4345.
9. Schnaper, H. W., T. Hayashida, S. C. Hubchak, and A. C. Poncelet. 2003. TGF-beta signal transduction and mesangial cell fibrogenesis. *Am. J. Physiol. Renal Physiol.* 284: F243–F252.
10. Poncelet, A. C., and H. W. Schnaper. 1998. Regulation of human mesangial cell collagen expression by transforming growth factor-beta1. *Am. J. Physiol.* 275: F458–F466.
11. Islam, M., J. F. Burke, Jr., T. A. McGowan, Y. Zhu, S. R. Dunn, P. McCue, J. Kanalas, and K. Sharma. 2001. Effect of anti-transforming growth factor-beta antibodies in cyclosporine-induced renal dysfunction. *Kidney Int.* 59: 498–506.
12. Hänsch, G. M., C. Wagner, A. Bürger, W. Dong, G. Staehler, and M. Stoeck. 1995. Matrix protein synthesis by glomerular mesangial cells in culture: effects of transforming growth factor beta (TGF beta) and platelet-derived growth factor (PDGF) on fibronectin and collagen type IV mRNA. *J. Cell. Physiol.* 163: 451–457.
13. Gupta, S., M. R. Clarkson, J. Duggan, and H. R. Brady. 2000. Connective tissue growth factor: potential role in glomerulosclerosis and tubulointerstitial fibrosis. *Kidney Int.* 58: 1389–1399.
14. Akool, S., A. Doller, A. Babelova, W. Tsalastra, K. Moreth, L. Schaefer, J. Pfeilschifter, and W. Eberhardt. 2008. Molecular mechanisms of TGF beta receptor-triggered signaling cascades rapidly induced by the calcineurin inhibitors cyclosporin A and FK506. *J. Immunol.* 181: 2831–2845.
15. Lu, Z. H., J. T. Books, and T. J. Ley. 2005. YB-1 is important for late-stage embryonic development, optimal cellular stress responses, and the prevention of premature senescence. *Mol. Cell. Biol.* 25: 4625–4637.
16. Schittek, B., K. Psenner, B. Sauer, F. Meier, T. Iftner, and C. Garbe. 2007. The increased expression of Y box-binding protein 1 in melanoma stimulates proliferation and tumor invasion, antagonizes apoptosis and enhances chemoresistance. *Int. J. Cancer* 120: 2110–2118.
17. Fraser, D. J., A. O. Phillips, X. Zhang, C. R. van Roeyen, P. Muehlenberg, A. En-Nia, and P. R. Mertens. 2008. Y-box protein-1 controls transforming growth factor-beta1 translation in proximal tubular cells. *Kidney Int.* 73: 724–732.
18. Raffetseder, U., B. Frye, T. Rauen, K. Jürchott, H. D. Royer, P. L. Jansen, and P. R. Mertens. 2003. Splicing factor SRp30c interaction with Y-box protein-1 confers nuclear YB-1 shuttling and alternative splice site selection. *J. Biol. Chem.* 278: 18241–18248.
19. Norman, J. T., G. E. Lindahl, K. Shakib, A. En-Nia, E. Yilmaz, and P. R. Mertens. 2001. The Y-box binding protein YB-1 suppresses collagen alpha 1(I) gene transcription via an evolutionarily conserved regulatory element in the proximal promoter. *J. Biol. Chem.* 276: 29880–29890.
20. Mertens, P. R., S. Harendza, A. S. Pollock, and D. H. Lovett. 1997. Glomerular mesangial cell-specific transactivation of matrix metalloproteinase 2 transcription is mediated by YB-1. *J. Biol. Chem.* 272: 22905–22912.
21. Raffetseder, U., T. Rauen, S. Djudjaj, M. Kretzler, A. En-Nia, F. Tacke, H. W. Zimmermann, P. J. Nelson, B. C. Frye, J. Floege, et al. 2009. Differential regulation of chemokine CCL5 expression in monocytes/macrophages and renal cells by Y-box protein-1. *Kidney Int.* 75: 185–196.
22. Krohn, R., U. Raffetseder, I. Bot, A. Zernecke, E. Shagdarsuren, E. A. Liehn, P. J. van Santbrink, P. J. Nelson, E. A. Biessen, P. R. Mertens, and C. Weber. 2007. Y-box binding protein-1 controls CC chemokine ligand-5 (CCL5) expression in smooth muscle cells and contributes to neointima formation in atherosclerosis-prone mice. *Circulation* 116: 1812–1820.
23. Rauen, T., U. Raffetseder, B. C. Frye, S. Djudjaj, P. J. Mühlenberg, F. Eitner, U. Lendahl, J. Bernhagen, S. Dooley, and P. R. Mertens. 2009. YB-1 acts as a ligand for Notch-3 receptors and modulates receptor activation. *J. Biol. Chem.* 284: 26928–26940.
24. van Roeyen, C. R., F. Eitner, S. Martinkus, S. R. Thieltges, T. Ostendorf, D. Bokemeyer, B. Lüscher, J. M. Lüscher-Firzlaff, J. Floege, and P. R. Mertens. 2005. Y-box protein 1 mediates PDGF-B effects in mesangioproliferative glomerular disease. *J. Am. Soc. Nephrol.* 16: 2985–2996.
25. Feng, Q., S. Huang, A. Zhang, Q. Chen, X. Guo, R. Chen, and T. Yang. 2009. Y-box protein 1 stimulates mesangial cell proliferation via activation of ERK1/2. *Nephron, Exp. Nephrol.* 113: e16–e25.
26. Zhang, A., X. Liu, J. G. Cogan, M. D. Fuerst, J. A. Polikandriotis, R. J. Kelm, Jr., and A. R. Strauch. 2005. YB-1 coordinates vascular smooth muscle alpha-actin gene activation by transforming growth factor beta1 and thrombin during differentiation of human pulmonary myofibroblasts. *Mol. Biol. Cell* 16: 4931–4940.
27. Higashi, K., Y. Inagaki, K. Fujimori, A. Nakao, H. Kaneko, and I. Nakatsuka. 2003. Interferon-gamma interferes with transforming growth factor-beta signaling through direct interaction of YB-1 with Smad3. *J. Biol. Chem.* 278: 43470–43479.
28. Higashi, K., Y. Inagaki, N. Suzuki, S. Mitsui, A. Mauviel, H. Kaneko, and I. Nakatsuka. 2003. Y-box-binding protein YB-1 mediates transcriptional repression of human alpha 2(I) collagen gene expression by interferon-gamma. *J. Biol. Chem.* 278: 5156–5162.
29. Sun, W., F. Hou, M. P. Panchenko, and B. D. Smith. 2001. A member of the Y-box protein family interacts with an upstream element in the alpha1(I) collagen gene. *Matrix Biol.* 20: 527–541.
30. Mundel, P., J. Reiser, A. Zúñiga Mejía Borja, H. Pavenstädt, G. R. Davidson, W. Kriz, and R. Zeller. 1997. Rearrangements of the cytoskeleton and cell contacts induce process formation during differentiation of conditionally immortalized mouse podocyte cell lines. *Exp. Cell Res.* 236: 248–258.
31. Sawada, S., G. Suzuki, Y. Kawase, and F. Takaku. 1987. Novel immunosuppressive agent, FK506. In vitro effects on the cloned T cell activation. *J. Immunol.* 139: 1797–1803.
32. Sorokin, A. V., A. A. Selyutina, M. A. Skabkin, S. G. Guryanov, I. V. Nazimov, C. Richard, J. Th'ng, J. Yau, P. H. Sorensen, L. P. Ovchinnikov, and V. Evdokimova. 2005. Proteasome-mediated cleavage of the Y-box-binding protein 1 is linked to DNA-damage stress response. *EMBO J.* 24: 3602–3612.
33. Krauskopf, A., T. M. Buetler, N. S. Nguyen, K. Macé, and U. T. Ruegg. 2002. Cyclosporin A-induced free radical generation is not mediated by cytochrome P-450. *Br. J. Pharmacol.* 135: 977–986.
34. Coles, L. S., L. Lambrusco, J. Burrows, J. Hunter, P. Diamond, A. G. Bert, M. A. Vadas, and G. J. Goodall. 2005. Phosphorylation of cold shock domain/Y-box proteins by ERK2 and GSK3beta and repression of the human VEGF promoter. *FEBS Lett.* 579: 5372–5378.
35. Stratford, A. L., C. J. Fry, C. Desilets, A. H. Davies, Y. Y. Cho, Y. Li, Z. Dong, I. M. Berquin, P. P. Roux, and S. E. Dunn. 2008. Y-box binding protein-1 serine 102 is a downstream target of p90 ribosomal S6 kinase in basal-like breast cancer cells. *Breast Cancer Res.* 10: R99.
36. Evdokimova, V., P. Ruzanov, M. S. Anglesio, A. V. Sorokin, L. P. Ovchinnikov, J. Buckley, T. J. Triche, N. Sonenberg, and P. H. Sorensen. 2006. Akt-mediated YB-1 phosphorylation activates translation of silent mRNA species. *Mol. Cell. Biol.* 26: 277–292.
37. Sutherland, B. W., J. Kucab, J. Wu, C. Lee, M. C. Cheang, E. Yorida, D. Turbin, S. Dedhar, C. Nelson, M. Pollak, et al. 2005. Akt phosphorylates the Y-box binding protein 1 at Ser102 located in the cold shock domain and affects the anchorage-independent growth of breast cancer cells. *Oncogene* 24: 4281–4292.
38. Basu, A., D. Datta, D. Zurakowski, and S. Pal. 2010. Altered VEGF mRNA stability following treatments with immunosuppressive agents: implications for cancer development. *J. Biol. Chem.* 285: 25196–25202.
39. Liu, Y. 2006. Renal fibrosis: new insights into the pathogenesis and therapeutics. *Kidney Int.* 69: 213–217.
40. Ishimura, E., R. B. Sterzel, H. Morii, and M. Kashgarian. 1992. Extracellular matrix protein: gene expression and synthesis in cultured rat mesangial cells. *Nippon Jinzo Gakkai Shi* 34: 9–17.

41. Kashgarian, M., and R. B. Sterzel. 1992. The pathobiology of the mesangium. *Kidney Int.* 41: 524–529.
42. Matsumoto, K., S. Abiko, and H. Ariga. 2005. Transcription regulatory complex including YB-1 controls expression of mouse matrix metalloproteinase-2 gene in NIH3T3 cells. *Biol. Pharm. Bull.* 28: 1500–1504.
43. Dooley, S., H. M. Said, A. M. Gressner, J. Floege, A. En-Nia, and P. R. Mertens. 2006. Y-box protein-1 is the crucial mediator of antifibrotic interferon-gamma effects. *J. Biol. Chem.* 281: 1784–1795.
44. Uchiumi, T., A. Fotovati, T. Sasaguri, K. Shibahara, T. Shimada, T. Fukuda, T. Nakamura, H. Izumi, T. Tsuzuki, M. Kuwano, and K. Kohno. 2006. YB-1 is important for an early stage embryonic development: neural tube formation and cell proliferation. *J. Biol. Chem.* 281: 40440–40449.
45. Lally, C., E. Healy, and M. P. Ryan. 1999. Cyclosporine A-induced cell cycle arrest and cell death in renal epithelial cells. *Kidney Int.* 56: 1254–1257.
46. Jennings, P., C. Koppelstaetter, S. Aydin, T. Abberger, A. M. Wolf, G. Mayer, and W. Pfaller. 2007. Cyclosporine A induces senescence in renal tubular epithelial cells. *Am. J. Physiol. Renal Physiol.* 293: F831–F838.
47. Duh, J. L., H. Zhu, H. G. Shertzer, D. W. Nebert, and A. Puga. 1995. The Y-box motif mediates redox-dependent transcriptional activation in mouse cells. *J. Biol. Chem.* 270: 30499–30507.
48. Satriano, J. A., B. Banas, B. Luckow, P. Nelson, and D. O. Schlondorff. 1997. Regulation of RANTES and ICAM-1 expression in murine mesangial cells. *J. Am. Soc. Nephrol.* 8: 596–603.
49. Coronella-Wood, J., J. Terrand, H. Sun, and Q. M. Chen. 2004. c-Fos phosphorylation induced by H2O2 prevents proteasomal degradation of c-Fos in cardiomyocytes. *J. Biol. Chem.* 279: 33567–33574.
50. Faul, C., M. Donnelly, S. Merscher-Gomez, Y. H. Chang, S. Franz, J. Delfgaauw, J. M. Chang, H. Y. Choi, K. N. Campbell, K. Kim, et al. 2008. The actin cytoskeleton of kidney podocytes is a direct target of the antiproteinuric effect of cyclosporine A. *Nat. Med.* 14: 931–938.
51. Skabkin, M. A., O. I. Kiselyova, K. G. Chernov, A. V. Sorokin, E. V. Dubrovin, I. V. Yaminsky, V. D. Vasiliev, and L. P. Ovchinnikov. 2004. Structural organization of mRNA complexes with major core mRNP protein YB-1. *Nucleic Acids Res.* 32: 5621–5635.
52. Evdokimova, V., P. Ruzanov, H. Imataka, B. Raught, Y. Svitkin, L. P. Ovchinnikov, and N. Sonenberg. 2001. The major mRNA-associated protein YB-1 is a potent 5′ cap-dependent mRNA stabilizer. *EMBO J.* 20: 5491–5502.
53. Evdokimova, V., C. Tognon, T. Ng, P. Ruzanov, N. Melnyk, D. Fink, A. Sorokin, L. P. Ovchinnikov, E. Davicioni, T. J. Triche, and P. H. Sorensen. 2009. Translational activation of snail1 and other developmentally regulated transcription factors by YB-1 promotes an epithelial-mesenchymal transition. *Cancer Cell* 15: 402–415.
54. Evdokimova, V., L. P. Ovchinnikov, and P. H. Sorensen. 2006. Y-box binding protein 1: providing a new angle on translational regulation. *Cell Cycle* 5: 1143–1147.
55. Hayashida, T., A. C. Poncelet, S. C. Hubchak, and H. W. Schnaper. 1999. TGF-beta1 activates MAP kinase in human mesangial cells: a possible role in collagen expression. *Kidney Int.* 56: 1710–1720.
56. Pontrelli, P., M. Rossini, B. Infante, G. Stallone, A. Schena, A. Loverre, M. Ursi, R. Verrienti, A. Maiorano, G. Zaza, et al. 2008. Rapamycin inhibits PAI-1 expression and reduces interstitial fibrosis and glomerulosclerosis in chronic allograft nephropathy. *Transplantation* 85: 125–134.